

This item is likely protected under Title 17 of the U.S. Copyright Law. Unless on a Creative Commons license, for uses protected by Copyright Law, contact the copyright holder or the author.

Access to this work was provided by the University of Maryland, Baltimore County (UMBC) ScholarWorks@UMBC digital repository on the Maryland Shared Open Access (MD-SOAR) platform.

Please provide feedback

Please support the ScholarWorks@UMBC repository by emailing scholarworks-group@umbc.edu and telling us what having access to this work means to you and why it's important to you. Thank you.

RXTE DISCOVERY OF MULTIPLE CYCLOTRON LINES DURING THE 2004 DECEMBER OUTBURST OF V0332+53

KATJA POTTSCHMIDT,¹ INGO KREYKENBOHM,^{2,3} JÖRN WILMS,⁴ WAYNE COBURN,⁵ RICHARD E. ROTHSCILD,¹
 PETER KRETSCHMAR,⁶ VANESSA MCBRIDE,⁷ SLAWOMIR SUCHY,¹ AND RÜDIGER STAUBERT²

Received 2005 June 24; accepted 2005 October 10; published 2005 November 2

ABSTRACT

We present an analysis of the 2–150 keV spectrum of the transient X-ray pulsar V0332+53 taken with the *Rossi X-Ray Timing Explorer* (RXTE) in 2004 December. We report on the detection of three cyclotron resonance features at 27, 51, and 74 keV in the phase-averaged data, corresponding to a polar magnetic field of 2.7×10^{12} G. After 4U 0115+63, this makes V0332+53 the second accreting neutron star in which more than two cyclotron lines have been detected; this has now also been confirmed by *INTEGRAL*. Pulse-phase spectroscopy reveals remarkably little variability of the cyclotron line through the 4.4 s X-ray pulse.

Subject headings: pulsars: individual (V0332+53) — stars: flare — stars: magnetic fields — X-rays: binaries — X-rays: stars

Online material: color figures

1. INTRODUCTION

The recurring transient X-ray pulsar V0332+53 was discovered in 1983 in *Tenma* observations made from 1983 November to 1984 January (Tanaka 1983; Makishima et al. 1990b). Subsequently, an outburst was revealed in *Vela 5B* data to have occurred in 1973 summer (Terrell et al. 1983; Terrell & Priedhorsky 1984). In rapid follow-up observations to the *Tenma* detection by *EXOSAT* during the 1983 outburst, 4.4 s pulsations were discovered, an accurate position was determined, and indications were found for an orbital period of 34.25 days (Stella et al. 1985). The position and subsequent optical/X-ray variability secured the identification of the counterpart with the heavily reddened B star BQ Cam (Argyle et al. 1983). Later investigations refined the spectral type to O8–9 (Negueruela et al. 1999).

Analysis of the *Tenma* data revealed a shape similar to that seen in other accreting X-ray pulsars with a flat power law and exponential cutoff, and also showed evidence of a cyclotron line at ~28 keV (Makishima et al. 1990b). In 1989 September the source experienced another outburst, this time observed by *Ginga* (Makino 1989). With the energy range of the Large Area Counters adjusted to cover the 2–60 keV range, cyclotron resonant scattering features (CRSF) were detected at 28.5 and 53 keV (Makishima et al. 1990a). At the time, this was the fourth accreting X-ray pulsar system to exhibit cyclotron features. Since then a significant number of this class of objects have been shown to have CRSFs, with 4U 0115+63 setting the record for the number of harmonics at five (see Heindl et al. 2004 for a review).

V0332+53 went into outburst again in 2004 November, reaching a 1.5–12 keV intensity of ~1 crab (Remillard 2004).

A long series of observations by the Proportional Counter Array (PCA; Jahoda et al. 2005)⁸ and High-Energy X-Ray Timing Experiment (HEXTE; Rothschild et al. 1998) aboard RXTE were made throughout the outburst. Following up on our initial announcement (Coburn et al. 2005), here we report the discovery of a third cyclotron line at ~74 keV, along with clear evidence for a non-Gaussian shape of the fundamental. In § 2 we present the observations and the data extraction. The phase-averaged and the phase-resolved spectra are analyzed and discussed in § 3 and § 4, respectively. In § 5 we summarize the results and present our conclusions.

2. OBSERVATIONS AND DATA EXTRACTION

Since the luminosity of the source is strongly variable during the outburst, we decided to concentrate on the three longest observations during the peak of the outburst as observed in the soft X-ray band by the RXTE All Sky Monitor (ASM; Fig. 1). Results from the full monitoring data set will be presented elsewhere. We combined the PCA and HEXTE data taken 2004 December 24–26 (RXTE ObsIDs 90089-11-05-08G, 90089-22-01-00G, and 90089-22-01-01G), giving a total of ~58 ks of exposure in the PCA and 14.4 ks of dead-time-corrected live time in HEXTE cluster B. At the time of the selected observations, HEXTE’s cluster A was not rocking due to a single event upset, and we discarded data from this cluster.⁹ The data were reduced with HEASOFT version 5.3.1, and spectral modeling was performed with XSPEC version 11.3.1w (Arnaud 1996). For modeling the phase-averaged spectra (Fig. 2a), PCA data from 3–20 keV and HEXTE data from 18–150 keV were used, and the HEXTE data were rebinned by factors of 3 and 5 between 70–100 and 100–150 keV, respectively. A systematic error of 0.5% was assumed for the PCA.

3. PHASE-AVERAGED SPECTRA

The X-ray spectrum observed from accreting X-ray pulsars is the superposition of X-rays originating in the accretion column and the hot spots on the surface of the neutron star. The neutron star’s X-rays are partially intercepted by the material present in the system, such as the stellar wind, giving rise to

¹ University of California, San Diego, Center for Astrophysics and Space Sciences, 9500 Gilman Drive, La Jolla, CA 92093-0424; kpottschmidt@ucsd.edu, rrothschild@ucsd.edu, ssuchy@ucsd.edu.

² Institut für Astronomie und Astrophysik, Astronomy Section, Sand 1, 72076 Tübingen, Germany; staubert@astro.uni-tuebingen.de.

³ INTEGRAL Science Data Centre, Chemin d’Écogia 16, 1290 Versoix, Switzerland; ingo.kreykenbohm@obs.unige.ch.

⁴ Department of Physics, University of Warwick, Coventry CV4 7AL, UK; j.wilms@warwick.ac.uk.

⁵ Space Sciences Laboratory, University of California, Berkeley, CA 94702-7450; wcoburn@ssl.berkeley.edu.

⁶ European Space Agency, European Space Astronomy Centre, Villafraanca del Castillo, 28080 Madrid, Spain; peter.kretschmar@esa.int.

⁷ School of Physics and Astronomy, Southampton University, Southampton SO17 1BJ, UK; vanessa@astro.soton.ac.uk.

⁸ See also <http://heawww.gsfc.nasa.gov/docs/xray/xte/pca/>.

⁹ Cluster A was subsequently rebooted and continues to work normally.

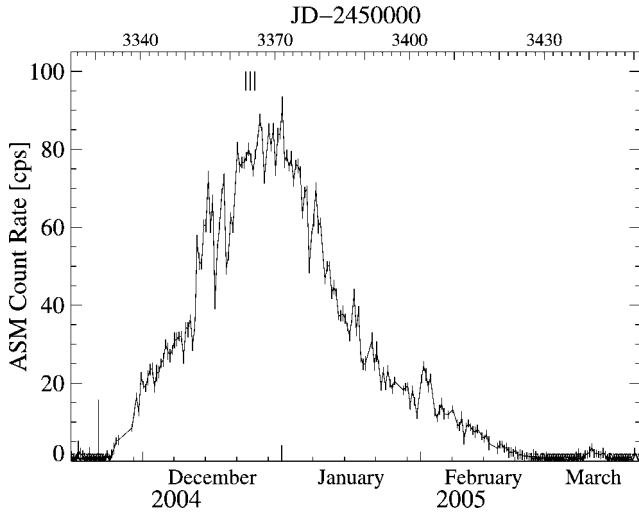


FIG. 1.—*RXTE* ASM 1.5–12 keV light curve of the 2004/2005 outburst of V0332+53, binned to 0.5 day resolution. Tick marks denote the times of the observations analyzed in this Letter.

significant absorption, which can exceed 10^{23} H atoms cm^{-2} (see, e.g., Becker & Wolff 2005 for a discussion of the formation of the X-ray continuum in the accretion column).

The $\mathcal{O}(10^{12}$ G) magnetic field close to the magnetic poles of the neutron star leads to the formation of CRSFs in the X-ray spectrum. The observer's frame energy of the CRSFs is given by (Mészáros 1992)

$$E_{C,n} = \frac{2nE_F}{1+z} \left(1 + \sqrt{1 + 2n \frac{E_F}{m_e c^2} \sin^2 \theta} \right)^{-1} \quad (1)$$

$$\sim \frac{nE_F}{1+z}, \quad (2)$$

where $n = 1, 2, \dots$, is the harmonic number, $E_F = (11.6 \text{ keV}) (B/10^{12} \text{ G})$ is the fundamental nonrelativistic cyclotron energy ($n = 1$), θ is the angle between the wavevector of the incoming photon and the magnetic field B , and $z \sim 0.3$ is the gravitational redshift (assuming a $1.4 M_\odot$ neutron star with a 10 km radius). The great importance of CRSF observations is that they provide the only direct way to measure neutron star B -field strengths.

The lack of adequate theoretical continuum models for accreting neutron stars necessitates the use of empirical models to describe the observations (Kreykenbohm et al. 1999). We use a power law modified at higher energies by a “Fermi-Dirac cutoff” (Tanaka 1986) to fit the PCA and HEXTE data simultaneously, including a multiplicative constant as a fitting parameter to allow for the slight difference ($\leq 5\%$) in the flux calibration of both instruments. Photoelectric absorption and a strong Fe $K\alpha$ fluorescence line at 6.35 keV from neutral iron, with a width of $\sigma_{\text{Fe}K\alpha} = 0.43$ keV and an equivalent width of 123 eV are also taken into account. The soft continuum parameters found (see below) are in general agreement with earlier results (e.g., Unger et al. 1992).

While this model fits the overall shape of the continuum reasonably well, strong absorption-like features are present

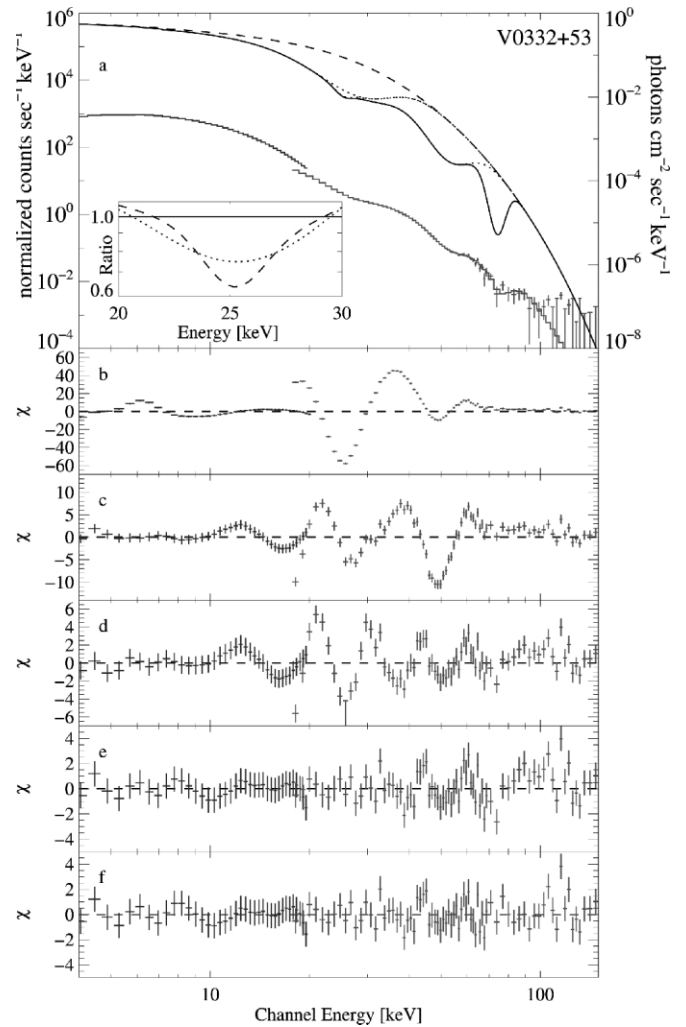


FIG. 2.—Cyclotron line modeling of the phase-averaged PCA/HEXTE spectrum of V0332+53. (a) Combined PCA/HEXTE spectrum (crosses), best-fit model (histogram), and unfolded spectrum (dotted and solid lines, right y-axis label), illustrating the cumulative effect of the CRSFs on the continuum (see text for a description of the continuum model). Note that the lines are already visible in the raw count spectrum. The inset shows the best-fit spectra with one (dotted line) and two (dashed line) line components for the fundamental line relative to the best-fit continuum with no lines (solid line). Panels b–f show residuals for models taking different numbers of CRSFs into account (see Table 1 for the best-fit values). (b) No line; (c) one line at 25.5 keV; (d) two lines, one at 26.6 keV and one at 50 keV; (e) two lines, a fundamental line that is best modeled with two Gaussian components at 25.2 and 26.6 keV and its harmonic at 49.9 keV; (f) three lines, the fundamental modeled by two components at ~ 25 and ~ 27 keV, and two lines at ~ 51 and ~ 74 keV. [See the electronic edition of the Journal for a color version of this figure.]

above 20 keV (Fig. 2b), which we model as lines with Gaussian optical depth profiles of the form

$$\tau(E) = \tau_c \exp \left[-\frac{1}{2} \left(\frac{E - E_c}{\sigma_c} \right)^2 \right], \quad (3)$$

where E_c is the line energy, σ_c is the line width, and τ_c is the optical depth at the line center. The spectral shape is then given by multiplying the continuum spectrum by $\exp[-\tau(E)]$ (Kreykenbohm et al. 2004, and references therein).

We start by modeling the strongest feature between 20 and 30 keV with one of these Gaussian components (see Table 1 for the relevant best-fit parameters). This feature corresponds to the CRSF first reported by Makishima et al. (1990a). While the 20–

TABLE 1
SPECTRAL PARAMETERS FOR THE PHASE-AVERAGED SPECTRUM

Parameter	2c	2d	2e	2f
N_H (10^{22} cm^{-2})	$0.0^{+0.2}_{-0.0}$	$1.3^{+0.5}_{-0.3}$	$1.5^{+0.5}_{-0.7}$	$1.6^{+0.6}_{-0.6}$
Γ	$-0.16^{+0.02}_{-0.01}$	$0.04^{+0.04}_{-0.03}$	$0.37^{+0.07}_{-0.05}$	$0.42^{+0.05}_{-0.05}$
E_{cut} (keV)	$0.0^{+0.1}_{-0.0}$	$0.0^{+0.7}_{-0.0}$	$13.0^{+3.2}_{-4.2}$	$17.2^{+3.2}_{-4.6}$
E_{fold} (keV)	$6.1^{+0.0}_{-0.0}$	$7.1^{+0.2}_{-0.1}$	$7.0^{+0.2}_{-0.2}$	$8.0^{+0.7}_{-0.5}$
$E_{\text{cyc, 1a}}$ (keV)	$25.5^{+0.0}_{-0.0}$	$26.3^{+0.1}_{-0.1}$	$26.6^{+0.1}_{-0.1}$	$27.1^{+0.2}_{-0.1}$
$\sigma_{\text{cyc, 1a}}$ (keV)	$4.7^{+0.0}_{-0.0}$	$5.5^{+0.1}_{-0.1}$	$7.0^{+0.5}_{-0.3}$	$7.6^{+0.2}_{-0.2}$
$\tau_{\text{cyc, 1a}}$	$1.02^{+0.01}_{-0.01}$	$1.22^{+0.03}_{-0.04}$	$1.38^{+0.20}_{-0.11}$	$1.81^{+0.08}_{-0.06}$
$E_{\text{cyc, 1b}}$ (keV)	$25.2^{+0.2}_{-0.2}$	$25.2^{+0.2}_{-0.2}$
$\sigma_{\text{cyc, 1b}}$ (keV)	$1.3^{+0.5}_{-0.5}$	$1.5^{+0.3}_{-0.5}$
$\tau_{\text{cyc, 1b}}$	$0.35^{+0.13}_{-0.04}$	$0.34^{+0.09}_{-0.03}$
$E_{\text{cyc, 2}}$ (keV)	...	$50.0^{+0.4}_{-0.4}$	$49.9^{+0.4}_{-0.3}$	$51.3^{+0.4}_{-0.4}$
$\sigma_{\text{cyc, 2}}$ (keV)	...	$6.5^{+0.5}_{-0.3}$	$6.5^{+0.5}_{-0.5}$	$8.9^{+0.6}_{-0.6}$
$\tau_{\text{cyc, 2}}$...	$0.94^{+0.09}_{-0.09}$	$1.19^{+0.14}_{-0.11}$	$2.21^{+0.31}_{-0.26}$
$E_{\text{cyc, 3}}$ (keV)	$73.7^{+1.5}_{-1.3}$
$\sigma_{\text{cyc, 3}}$ (keV)	$4.5^{+2.5}_{-2.7}$
$\tau_{\text{cyc, 3}}$	$3.3^{+2.6}_{-1.1}$
$\chi^2_{\text{red}}/\text{dof}$	16.24/104	4.05/101	1.37/98	1.04/95

NOTES.—The columns refer to residuals shown in Fig. 2. Symbols denote the equivalent hydrogen column, N_H , the photon index, Γ , the cutoff and folding energies of the Fermi-Dirac continuum, E_{cut} and E_{fold} , and the cyclotron line parameters E_{cyc} , σ_{cyc} , and τ_{cyc} (defined in eq. [3]) for fits with 1, 2, and 3 CRSFs. CRSF parameters labeled 1a and 1b correspond to the complex profile of the fundamental line. See text for a description of the continuum model. χ^2_{red} is the reduced χ^2 and dof is the number of degrees of freedom. All uncertainties are 90% confidence levels for one interesting parameter ($\Delta\chi^2 = 2.71$).

30 keV residuals improve significantly compared to the pure continuum fit when this component is included, another strong and remarkably well-defined absorption-like feature emerges at ~ 50 keV (Fig. 2c). This feature is the first harmonic of the cyclotron line, found at ~ 2 times the energy of the fundamental and already tentatively reported by Makishima et al. (1990a). Taking these two lines into account, weaker residuals remain at ~ 25 keV (Fig. 2d). Similar to 4U 0115+63 (Heindl et al. 1999) and other sources, these residuals are caused by the fundamental CRSF having a nontrivial shape, which cannot be modeled well with any simple line shape (see § 5). To describe the complex shape we add a shallow ($\tau_{\text{cyc, 1b}} \sim 0.3$) and narrow ($\sigma_{\text{cyc, 1b}} \sim 1.5$ keV) line component at an energy similar to that of the fundamental, $E_{\text{cyc, 1b}} = 25.2^{+0.2}_{-0.2}$ keV; the shape of this more complex line profile is shown in the inset of Figure 2a. Although lowering the χ^2 considerably, the fit is still not acceptable, and significant residuals remain (Fig. 2e). Adding another line at $73.7^{+1.5}_{-1.3}$ keV improves the fit significantly to $\chi^2_{\text{red}} = 1.04$ (Fig. 2f; the unfolded spectrum and the consecutive effect of the individual CRSFs are shown in Fig. 2a). The F -test probability that this improvement is due to chance is only 3×10^{-6} (however, see Protassov et al. 2002 concerning the applicability of the F -test in this case).

To verify the detection of the CRSFs and to confirm their independence from the choice of the continuum, we modeled the data with other continua commonly used to describe the spectra of accreting pulsars. The negative-positive exponential continuum (NPEX, Mihara 1995), for example, also requires the presence of three CRSFs at 27, 51.7, and 74.8 keV, again with a non-Gaussian fundamental. Other continua gave similar results, as do other prescriptions for the shape of the CRSF. The actual choice of the continuum or line shape is thus irrelevant for the detection and characterization of the CRSFs at the level of the *RXTE* energy resolution. We therefore report the discovery of the second harmonic of the cyclotron line in V0332+53 with *RXTE*, confirming our preliminary initial report for this data set (Coburn et al. 2005). This discovery has

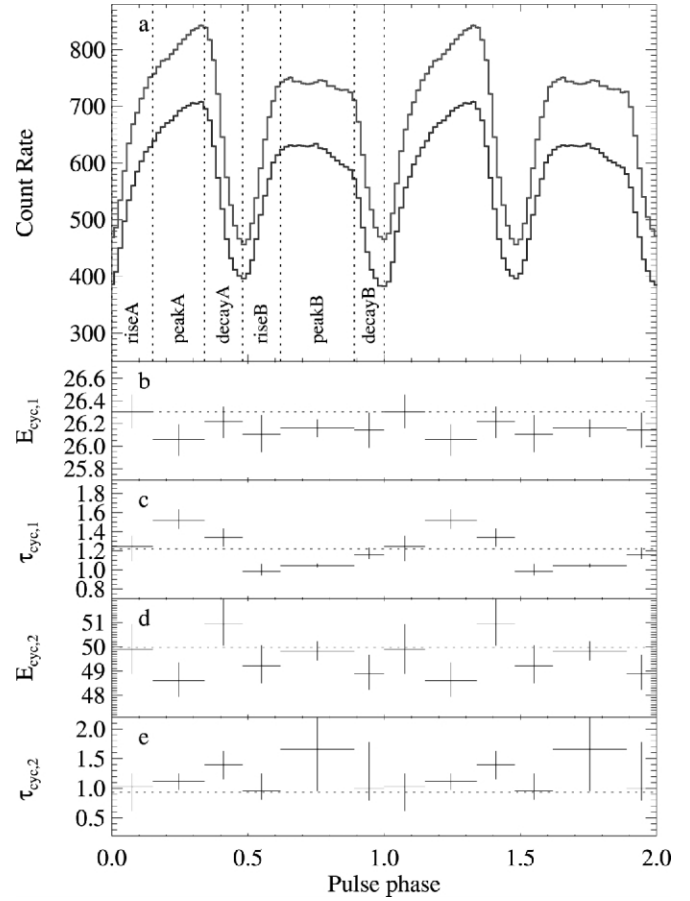


FIG. 3.—Pulse profile and CRSF variability of V0332+53. (a) HEXTE (full band, upper profile) and PCA (20–50 keV; lower profile) pulse profile. Also shown are the phase evolution of (b) the energy and the depth of (c) the fundamental and (d, e) the first harmonic cyclotron line. Error bars are at the 90% level for one interesting parameter; dotted lines indicate the best-fit values from the two CRSF fit to the phase averaged spectrum. [See the electronic edition of the Journal for a color version of this figure.]

been independently confirmed by subsequent *INTEGRAL* observations (Kreykenbohm et al. 2005).

4. PHASE-RESOLVED SPECTRA

The neutron star's magnetic axis is offset from its spin axis, not only giving rise to X-ray pulsations but also confronting the observer with a complex situation. Due to the rotation of the neutron star, the accretion column and the hot spots are seen under a constantly changing viewing angle. Since the physical conditions are likely to be variable within the emission region and since the CRSF line shape depends on the viewing angle, we expect the X-ray continuum and line parameters to depend on the pulse phase (Araya-Gómez & Harding 2000; Araya & Harding 1999; Isenberg et al. 1998). This has been confirmed by pulse-phase-resolved spectroscopy in a number of sources, such as GX 301–2 (Kreykenbohm et al. 2004, finding $\sim 20\%$ change in the line energy), Vela X-1 (Kreykenbohm et al. 2002; La Barbera et al. 2003), or 4U 0115+63 (Mihara et al. 2004).

To obtain phase-resolved spectra, we determined the pulse period for each of the three observations using standard techniques. This approach is necessary, as the accumulated uncertainty of the only available orbital ephemeris of the neutron star (Stella et al. 1985) is too large to allow any meaningful orbit correction. The average nonorbit-corrected X-ray period is $P = 4.3745$ s. After phase-aligning the resulting pulse pro-

files, we determined phase-resolved spectra. Figure 3a shows the resulting HEXTE and PCA pulse profile of V0332+53.

Since the data modes of the observation do not contain a PCA data mode with energy resolution below 20 keV and a sufficiently high time resolution for phase-resolved spectroscopy, we performed phase-resolved spectroscopy using the HEXTE data only. Signal-to-noise ratio considerations allow a maximum of six phase bins (Fig. 3a). In the resulting phase-resolved spectra, the source is detected to ~ 100 keV, such that we only model the lower two CRSFs and do not include the structure of the fundamental line. The absence of soft spectral data forces us to hold Γ and E_{cut} at the values found from the appropriate phase-averaged spectrum. This is justified by the relative constancy of these parameters as seen with earlier instruments (Unger et al. 1992). Both CRSFs are detected with high significance in all pulse phases. Figures 3b–3e show the evolution of the CRSF line energy and depth over the X-ray pulse. In contrast to the sources mentioned above, there is little to no variation in these parameters; no other spectral parameters show any significant variation either.

5. SUMMARY AND CONCLUSIONS

We have presented the discovery of a third cyclotron line in V0332+53, making this X-ray pulsar the second, after 4U 0115+63, with more than two cyclotron lines, and confirming the identification of the 26 keV line as the fundamental CRSF. Similar to sources such as 4U 0115+63 or GX 301–2, the HEXTE spectrum shows that the profile of the fundamental line has an asymmetric profile that is shallower toward lower energies. Such a profile is consistent with expectations from the asymmetric shape of the relativistic cross section for resonant electron scattering, but could also be influenced by the emission wings predicted in Monte Carlo simulations (Araya-Góchez & Harding 2000; Isenberg et al. 1998) or by a variation of the B -field in the emission region.

Consistent with the trend seen in most sources with multiple CRSFs, the energies of the fundamental and its harmonics do not scale like 1 : 2 : 3, as predicted by the nonrelativistic equation (2).

Rather, the line ratios are slightly smaller, in agreement with the prediction of relativistic quantum mechanics (eq. [1]). Using all three observed line energies (taking $E = 26.3$ keV for the fundamental line) and assuming $z = 0.3$, for V0332+53 a most probable polar magnetic field of 2.7×10^{12} G is found. Consistency between all three CRSF energies can only be reached for $\theta \gtrsim 60^\circ$; i.e., photons scattered out of the line have an initial direction that is perpendicular to the B -field, as is expected from the significant increase of the electron scattering cross section with $\theta \rightarrow 90^\circ$. This result provides a much stronger confirmation of the interpretation of the line features as CRSFs than is possible in sources where just the fundamental is observed.

Pulse-phase-resolved spectroscopy revealed that V0332+53 shows far less variability in the CRSF parameters than many other sources. The origin of the CRSF variability in these sources is unclear, although it has been pointed out that their complex pulse profiles make it likely that different regions of the accretion column or even different magnetic poles are seen during the X-ray pulse. The remarkably simple hard X-ray pulse profile of V0332+53 suggests a less complex accretion geometry than in other sources, which might also explain the very weak CRSF variability.

In conclusion, our observation of multiple lines strongly confirms the interpretation of these features as cyclotron lines. For a further interpretation of our results, however, more realistic models for the neutron star continuum and especially for the line shape are needed, to include the radiative transfer in the line, multiple photon scattering, etc., and thus also predict emission wings and strongly asymmetric profiles. Work is currently ongoing in our collaboration to compute such models for a variety of parameters to make such progress possible in the near future.

We thank both first referees for their remarks, which greatly improved this Letter. We acknowledge the support of NASA contract NAS5-30720, NASA grant NAG5-10691, NSF grants INT-9815741 and INT-0003773, and DLR grants 50OG9601, 50OG0501, and 50OR0302. V. McBride is funded jointly by the NRF (South Africa), British Council, and Southampton University.

REFERENCES

- Araya, R. A., & Harding, A. K. 1999, *ApJ*, 517, 334
 Araya-Góchez, R. A., & Harding, A. K. 2000, *ApJ*, 544, 1067
 Argyle, R. W., Kodaira, K., Bernacca, P. L., Iijima, T., & Stagni, R. 1983, *IAU Circ.*, 3897, 2
 Arnaud, K. A. 1996, in *ASP Conf. Ser. 101, Astronomical Data Analysis Software and Systems V*, ed. G. H. Jacoby & J. Barnes (San Francisco: ASP), 17
 Becker, P. A., & Wolff, M. T. 2005, *ApJ*, 621, L45
 Coburn, W., Kretschmar, P., Kreykenbohm, I., McBride, V. A., Rothschild, R. E., & Wilms, J. 2005, *Astron. Telegram*, 381, 1
 Heindl, W. A., Coburn, W., Gruber, D. E., Pelling, M. R., Rothschild, R. E., Wilms, J., Pottschmidt, K., & Staubert, R. 1999, *ApJ*, 521, L49
 Heindl, W. A., Rothschild, R. E., Coburn, W., Staubert, R., Wilms, J., Kreykenbohm, I., & Kretschmar, P. 2004, in *AIP Conf. Proc. 714, X-Ray Timing 2003: Rossi and Beyond*, ed. P. Kaaret, F. K. Lamb, & J. H. Swank (Melville: AIP), 323
 Isenberg, M., Lamb, D. Q., & Wang, J. C. L. 1998, *ApJ*, 493, 154
 Jahoda, K., Markwardt, C. B., Radeva, Y., Rots, A. H., Stark, M. J., Swank, J. H., Strohmayer, T. E., & Zhang, W. 2005, *ApJS*, submitted
 Kreykenbohm, I., Coburn, W., Wilms, J., Kretschmar, P., Staubert, R., Heindl, W. A., & Rothschild, R. E. 2002, *A&A*, 395, 129
 Kreykenbohm, I., Kretschmar, P., Wilms, J., Staubert, R., Kendziorra, E., Gruber, D. E., Heindl, W. A., & Rothschild, R. E. 1999, *A&A*, 341, 141
 Kreykenbohm, I., Wilms, J., Coburn, W., Kuster, M., Rothschild, R. E., Heindl, W. A., Kretschmar, P., & Staubert, R. 2004, *A&A*, 427, 975
 Kreykenbohm, I., et al. 2005, *A&A*, 433, L45
 La Barbera, A., Santangelo, A., Orlandini, M., & Segreto, A. 2003, *A&A*, 400, 993
 Makino, F. 1989, *IAU Circ.*, 4872, 2
 Makishima, K., et al. 1990a, *ApJ*, 365, L59
 ———. 1990b, *PASJ*, 42, 295
 Mészáros, P. 1992, *High-Energy Radiation from Magnetized Neutron Stars* (Chicago: Univ. Chicago Press)
 Mihara, T. 1995, Ph.D. thesis, RIKEN, Tokyo
 Mihara, T., Makishima, K., & Nagase, F. 2004, *ApJ*, 610, 390
 Negueruela, I., Roche, P., Fabregat, J., & Coe, M. J. 1999, *MNRAS*, 307, 695
 Protassov, R., van Dyk, D. A., Connors, A., Kashyap, V. L., & Siemiginowska, A. 2002, *ApJ*, 571, 545
 Remillard, R. 2004, *Astron. Telegram*, 371, 1
 Rothschild, R. E., et al. 1998, *ApJ*, 496, 538
 Stella, L., White, N. E., Davelaar, J., Parmar, A. N., Blissett, R. J., & van der Klis, M. 1985, *ApJ*, 288, L45
 Tanaka, Y. 1983, *IAU Circ.*, 3891, 2
 ———. 1986, in *Radiation Hydrodynamics in Stars and Compact Objects*, ed. D. Mihalas & K.-H. A. Winkler (Heidelberg: Springer), 198
 Terrell, J., & Priedhorsky, W. C. 1984, *ApJ*, 285, L15
 Terrell, J., et al. 1983, *IAU Circ.*, 3893, 1
 Unger, S. J., Norton, A. J., Coe, M. J., & Lehto, H. J. 1992, *MNRAS*, 256, 725